European Polymer Journal 45 (2009) 3326–3338

Contents lists available at ScienceDirect

European Polymer Journal

journal homepage: www.elsevier.com/locate/europolj

MACROMOLECULAR NANOTECHNOLOGY

Macromolecular Nanotechnology

Reaction-induced microphase separation in epoxy resin containing polystyrene-*block*-poly(ethylene oxide) alternating multiblock copolymer

Di Hu, Sixun Zheng *

Department of Polymer Science Engineering and State Key Laboratory of Metal Matrix Composites, Shanghai Jiao Tong University, Shanghai 200240, PR China

ARTICLE INFO

Article history:
Received 9 June 2009
Received in revised form 21 September 2009
Accepted 4 October 2009
Available online 9 October 2009

Keywords:
PS-*alt*-PEO alternating multiblock copolymer
Epoxy resin
Nanostructures
Reaction-induced microphase separation

ABSTRACT

Polystyrene-*block*-poly(ethylene oxide) alternating multiblock copolymer (PS-*alt*-PEO) was synthesized with the combination of atom transfer radical polymerization (ATRP) and Huisgen 1,3-dipolar cycloaddition (i.e., click chemistry). The copolymer has been characterized by means of Fourier transform infrared spectroscopy (FTIR), ^{1}H nuclear magnetic resonance spectroscopy (NMR), gel permeation chromatography (GPC) and differential scanning calorimetry (DSC). The PS-*alt*-PEO alternating multiblock copolymer was incorporated into epoxy resin to investigate the behavior of reaction-induced microphase separation, which has been compared to the case of the thermosets containing PS-*b*-PEO diblock copolymer. The morphology of epoxy thermosets containing PS-*alt*-PEO alternating multiblock copolymer were investigated by means of atomic force microscopy (AFM), and small-angle X-ray scattering (SAXS) and the nanostructures were detected in all the thermosetting blends investigated. In marked contrast to the case of the thermosets containing PS-*b*-PEO diblock copolymer, the thermosets containing PS-*alt*-PEO multiblock copolymer displayed disordered nanostructures, which have been interpreted on the basis of the restriction of the alternating multiblock topology of the block on the formation of the nanostructures *via* reaction-induced microphase separation.

1. Introduction

The formation of nanostructures in multi-component thermosets can further optimize the interactions between thermosetting matrix and modifiers and thus the mechanical properties of materials were significantly improved [1–5]. The concept of incorporating amphiphilic block copolymers into thermosets has widely been accepted to access ordered or disordered nanostructures in the materials [6–36]. Hillmyer et al. [6,7] have first reported the strategy of creating nanostructures *via* self-assembly approach. In the protocol, the precursors of thermosets act as the selective solvents of block copolymers and some self-assembly nanostructures such as lamellar, bicontinuous, cylindrical, and spherical structures are formed in the mixtures depending on the blend composition before curing reaction. These nanostructures can be further fixed *via* subsequent curing with introduction of hardeners. More recently, it was realized that ordered or disordered nanostructures in thermosets can be alternatively accessed *via* reaction-induced microphase separation (RIMS) mechanism [8,9]. In this mechanism, a part of subchains of the block copolymers were demixed with the occurrence of polymerization whereas the other subchains still remained miscible with the matrix of the thermosets.

It has been identified that the toughness improvement of the nanostructured thermosets are quite dependent on the morphology of the nanostructured thermosets in terms of the proposed toughening mechanisms such as debonding of micelles (or vesicles) from epoxy matrix, crack deflection and frictional interlocking for the thermosets possessing the terraced morphology [19,27] and matrix shear banding induced by nanocavitation [37–39]. It has provoked a considerable interest to control the formation of nanostructures in thermosets by the use of the block

---

* Corresponding author. Tel.: +86 21 54743278; fax: +86 21 54741297.
E-mail address: szheng@sjtu.edu.cn (S. Zheng).

0014-3057/$ - see front matter © 2009 Elsevier Ltd. All rights reserved.
doi:10.1016/j.eurpolymj.2009.10.001

copolymers with a variety of topological structures. During the past years, reactive or nonreactive AB diblock, ABA triblock and ABC triblock copolymers have been employed to access the ordered (or disordered) nanostructures in thermosets *via* self-assembly or reaction-induced microphase separation mechanisms [6–36]. It has been reported that epoxy-phobic subchains of these block copolymers can be dispersed in epoxy matrix in the form of spherical (e.g., micelle or vesicle), cylindrical (e.g., lamellar or wormlike) nanodomains.

In a previous work, we have reported the formation of ordered nanostructures in epoxy thermosets containing polystyrene-*block*-poly(ethylene oxide) (PS-*b*-PEO) diblock copolymer [8]. The curing reaction of epoxy resin started from the miscible mixtures comprised of precursors of epoxy and PS-*b*-PEO diblock copolymer. With the curing reaction proceeding, the PS blocks were gradually demixed *via* reaction-induced microphase separation mechanism. It was found that the nanophases of PS were arranged into a simple cubic symmetry lattices while the content of diblock copolymer was 40 wt.%. It is proposed that the formation of the ordered nanostructures is attributed to the structural feature of PS-*b*-PEO diblock copolymer. On the one hand, both PS and PEO blocks of the copolymer possess relatively narrow polydispersity of subchain length since they were prepared *via* cationic ring-opening polymerization (CROP) [40] and atom transfer radical polymerization (ATRP) [8]. The narrow distribution of molecular weights for the subchains could result that PS blocks formed the uniform nanodomains. On the other hand, in the diblock copolymer, each PS block possesses a single free end, i.e., the diblock topology of the copolymer could exert little restriction on the arrangement of PS nanodomain in epoxy matrix during the curing reaction. The structural effect on the formation of nanostructures in thermosets should be able to examine by changing the topological structures of block copolymer.

In this work, we synthesized polystyrene-*block*-poly(ethylene oxide) alternating multiblock copolymer (PS-*alt*-PEO) and this multiblock copolymer was then used to investigate the formation of the nanostructures in epoxy resin. To the best of our knowledge, alternating multiblock copolymers have less been involved although there are extensive reports on the formation of nanostructures in thermosets by the use of a variety of block copolymer during the past year [25]. The purpose of this work is to investigate the reaction-induced microphase separation of the alternating multiblock copolymer in epoxy resin and to examine the effect of multiblock topology on the nanostructures in thermosets. Toward this end, the PS-*alt*-PEO alternating block copolymer was synthesized *via* the combination of atom transfer radical polymerization (ATRP) and Huisgen 1,3-dipolar cycloaddition (i.e., click chemistry) [41–44]. The morphology of the nanostructured thermosets was investigated by means of differential scanning calorimetry (DSC), atomic force microscopy (AFM) and small-angle X-ray scattering (SAXS). The nanostructures were also compared to those of epoxy thermoset containing PS-*b*-PEO diblock copolymer, to underline the effect of topology of block copolymers on the formation of the nanostructures in the thermosets.

2. Experimental

2.1. Materials

Diglycidyl ether of bisphenol A (DGEBA) with epoxide equivalent weight of 185–210 was purchased from Shanghai Resin Co., China. 4,4′-Methylenebis (2-chloroaniline) (MOCA) was of analytically pure grade, obtained from Shanghai Reagent Co., China. Styrene (St) is of analytically pure grade and was purchased from Shanghai Reagent Co., China. Prior to use, the inhibitor was removed by washing with aqueous sodium hydroxide (5 wt.%) and deionized water and then the monomer was further dried with magnesium sulfate. Before use, the monomer was further distilled at reduced pressure. Dimethyl 2,6-dibromoheptanedioate was purchased from Aldrich Co., USA. Polyethylene glycol (PEG) was purchased from Fluka Co., Germany and it has a quote molecular weight of $M_n = 4000$. Poly(ethylene oxide) monomethyl ether (MPEO5000) with a quoted molecular weight of $M_n = 5000$ was purchased from Fluka Co., Germany and it was dried by azeotropic distillation with toluene prior to use. Copper (I) bromide (CuBr) was obtained from Shanghai Reagent Co., China and it was purified by successive washings with glacial acetic acid, methanol and then was dried under vacuum. *N,N,N′,N″,N″*-Pentamethyldiethylenetriamine (PMDETA) was purchased from Aldrich Co., USA and used as received. All other reagents and solvents used in this work are obtained from commercial resources and were purified according to standard procedures.

2.2. Synthesis of bromo-terminated polystyrene

Bromo-terminated polystyrene (Br-PS-Br) was prepared with atomic transfer radical polymerization (ATRP) and the complex of CuBr with *N,N,N′,N″,N″*-pentamethyldiethylenetriamine (PMDETA) was used as the catalyst and dimethyl 2,6-dibromoheptanedioate as the initiator according to the literature method [45]. Typically, dimethyl 2,6-dibromoheptanedioate (0.3339 g, 1 mmol), Cu(I)Br (0.0740 g, 0.5 mmol), PMDETA (102.86 μL, 0.5 mmol), and St (22.1733 g) were charged to a 50 mL round-bottom flask. The system was connected to the Schlenk line system, and three freeze–pump–thaw cycles were used to remove the trace of moisture and oxygen. The reactive system was immersed into an oil bath at 110 °C for 4 h. The crude product was dissolved in tetrahydrofuran and passed through a neutral alumina column to remove the catalyst; the polymer solution was concentrated and dropped into an excessive amount of cold methanol. The resulting product was dried *in vacuo* at 30 °C for 48 h. The polymer (4.7 g) was obtained by controlling the conversion of the monomer to be 21%. The molecular weight of the product was estimated by means of ^{1}H NMR spectroscopy in terms of the ratios of integration of protons in dimethyl 2,6-dibromoheptanedioate to that of styrene moiety. The molecular weight of the bromo-terminated PS is calculated to be $M_n = 4900$. The ^{1}H NMR ($CDCl_3$, ppm): 6.30–7.32 (215**H**, $C_6\boldsymbol{H}_5$), 4.3–4.65 (2**H**, $BrC\boldsymbol{H}CH_2$), 3.35–3.6 (6**H**, $\boldsymbol{H}_3COCO$).

2.3. Synthesis of azido-terminated polystyrene

To prepare diazido-terminated PS (N_3-PS-N_3), the above bromo-terminated PS (Br-PS-Br) (3.0 g, 1.2 mmol Br) was dissolved in *N*,*N*-dimethylformamide (48 mL) and NaN_3 (0.084 g, 1.3 mmol) was added. With continuous stirring, the reaction was carried out at 25 °C for 24 h. After precipitated into methanol, the resulting product was dried for 24 h in a vacuum oven at 30 °C and 2.75 g product was obtained with the yield of 95%. The ^1H NMR ($CDCl_3$, ppm): 6.30–7.32 (215**H**, $C_6\boldsymbol{H}_5$), 3.8–4.0 (2**H**, $N_3C\boldsymbol{H}CH_2$), 3.35–3.6 (6**H**, $\boldsymbol{H}_3COCO$).

2.4. Synthesis of propargyl-terminated poly(ethylene oxide)

In a nitrogen atmosphere, the appropriate PEG ($M_n = 4000$, 10 g, 4.0 mmol) in 66 mL anhydrous THF was added dropwise to a 150 mL Schlenk flask charged with NaH (0.384 g, 16 mmol). The reaction mixture was stirred for 0.5 h at ambient temperature; thereafter, propargyl bromide (1.904 g, 16 mmol) in 10 mL of THF was added slowly within 0.5 h. The reaction was carried out for additional 36 h at room temperature. Upon completion of the reaction, the mixture was filtered to remove insoluble solids, and the filtrate was concentrated *via* rotary evaporation and then dropped into a great amount of petroleum ether to afford the white precipitates. After dried at 30 °C in a vacuum oven for 24 h, the product (15.6 g) was obtained with the yield of 92%. The ^1H NMR ($CDCl_3$, ppm): 2.47 (2**H**, $\boldsymbol{H}CC$), 4.20 (4**H**, $HCC{-}C\boldsymbol{H}_2$), 3.63 (363**H**, $OC\boldsymbol{H}_2$-$C\boldsymbol{H}_2O$). FTIR (KBr window, cm^{-1}): 3244 (υ_s, H—C of alkyne).

2.5. Synthesis of PS-alt-PEO alternating multiblock copolymer by click chemistry

In a flask equipped with a magnetic stirring bar, azido-terminated polystyrene (N_3-PS-N_3) (5.0012 g, 1.00 mmol), propargyl-terminated poly(ethylene oxide) (4.278 g, 1.01 mmol), CuBr (143.0 mg, 1.00 mmol), and DMF-(90 mL) were added. The system was purged with highly pure nitrogen for 40 min and PMDETA (173.0 mg, 1.00 mmol) was then added. The click polymerization was carried out at 36 °C for 42 h. The reacted product was passed through neutral alumina column to remove copper salt, precipitated into cold ethyl ether, and dried under vacuum to give PS-*alt*-PEO. GPC: $M_n = 24{,}700$, $M_w = 55{,}190$. The ^1H NMR ($CDCl_3$, ppm): 3.35–3.6 (6**H**, $\boldsymbol{H}_3COCO$), 4.95–5.25 (1**H**, $C_6H_5{-}C\boldsymbol{H}{-}C_2HN_3$), 4.49–4.65 (2**H**, $C_2HN_3{-}C\boldsymbol{H}_2O$).

2.6. Synthesis of PS-b-PEO diblock copolymer

In order to synthesize PS-*b*-PEO diblock copolymer by means of atom transfer radical polymerization (ATRP), poly(ethylene oxide) macroinitiator was firstly prepared by following the literature method [46]. In this work, the poly(ethylene oxide) monomethyl ether with a quoted molecular weight of $M_n = 5000$ was used to react with 2-bromoisobutyryl bromide in the presence of triethylamine to afford the 2-bromoisobutyryl-ended PEO [PEO— $OOCCBr(CH_3)_2$]. The synthesis of diblock PS-*b*-PEO was carried out using a standard Schlenk line system. To a flask connected with the Schlenk line PEO-Br macroinitiator ($M_n = 5000$, 2.0 g, 0.4 mmol), CuBr (0.0576 g, 0.4 mmol), PMDETA (0.0693 g, 0.4 mmol) and styrene (4.0 g, 0.0385 mol) were charged. The reactive mixture was degassed *via* three pump freeze–thaw cycles and then immersed in a thermostated oil bath at 110 °C. After the polymerization was carried out for 10 h, the system was cooled to room temperature. Dichloromethane was added to dissolve the product. After filtered over a column of neutral alumina to remove the catalyst, the solution was dropped into an excessive amount of petroleum ether to afford the procipitates. The PS-*b*-PEO diblock copolymer was obtained and dried in a vacuum oven at room temperature for 24 h. The polymer (4.02 g) was obtained with a conversion of 50% for styrene monomer. FTIR) (KBr window): 2928(C—H, methylene of PEO), 1108 (C—O—C, ether of PEO), 1600, 1580, 1500 and 1450 (C═C of aromatic rings), 2922(C—H of PS), 3110–3010 (═C—H of aromatic rings). ^1H NMR ($CDCl_3$, ppm): 6.30–7.32 (protons of aromatic rings, 5H); 3.61 ($—OCH_2CH_2—$, 4H); 1.29–2.12 (protons of methylene and methane of PS subchain, 3H). GPC: $M_n = 10{,}100$, $M_w/M_n = 1.10$.

2.7. Preparation of epoxy thermosets containing PS-alt-PEO

The desired amount of PS-*alt*-PEO alternating multiblock copolymer (and/or PS-*b*-PEO diblock copolymer) was added to DGEBA with continuous stirring at 100 °C until the mixtures became homogenous and transparent. 4,4′-Methylene bis(2-chloroaniline) (MOCA) was added with continuous stirring until the full dissolution of the curing agent. The mixtures were poured into Teflon molds and cured at 150 °C for 2 h plus 180 °C for 2 h.

2.8. Measurements and characterization

2.8.1. Fourier transform infrared spectroscopy (FTIR)

The FTIR measurements were conducted on a Perkin Elmer Paragon 1000 Fourier transform infrared spectrometer at room temperature (25 °C). The spectra were obtained at the resolution of 2 cm^{-1} and were averages of 64 scans. The samples were granulated and the powder was mixed with KBr and then pressed into small flakes for FTIR measurement. All the specimens were sufficiently thin to be within a range where the Beer–Lambert law is obeyed.

2.8.2. Nuclear magnetic resonance spectroscopy (NMR)

The NMR measurements were carried out on a Varian Mercury Plus 400 MHz nuclear magnetic resonance spectrometer at 25 °C. The polymer was dissolved with deuterated chloroform and the ^1H NMR spectra were obtained with tetramethylsilane (TMS) as the internal reference.

2.8.3. Atomic force microscopy (AFM)

The specimens of thermosets for AFM observation were trimmed using a microtome machine, and the thickness of the specimens was about 70 nm. The morphological observation of the samples was conducted on a Nanoscope IIIa scanning probe microscope (Digital Instruments, Santa Barbara, CA) in tapping mode. A tip fabricated from silicon (125 μm in length with ca. 500 kHz resonant frequency) was used for scan, and the scan rate was 2.0 Hz.

2.8.4. Differential scanning calorimetry (DSC)

The thermal analysis was performed on a Perkin Elmer Pyris-1 differential scanning calorimeter in a dry nitrogen atmosphere. The instrument was calibrated with a standard Indium. The samples (about 10.0 mg in weight) were first heated up to 160 °C and held at this temperature for 3 min to eliminate thermal history, followed by quenching to −70 °C. To measure glass transition temperatures (T_g), a heating rate of 20 °C/min was used in all cases to observe clear transitions. Glass transition temperature (T_g) was taken as the midpoint of the heat capacity change.

2.8.5. Small-angle X-ray scattering (SAXS)

The SAXS measurements were taken on a Bruker Nanostar system. Two-dimensional diffraction patterns were recorded using an image intensified CCD detector. The experiments were carried out at room temperature (25 °C) using Cu KR radiation ($\lambda = 1.54$ Å, wavelength) operating at 40 kV, 35 mA. The intensity profiles were output as the plot of scattering intensity (I) *vs* scattering vector, $q = (4/\lambda)\sin(\theta/2)$ (θ = scattering angle).

2.8.6. Gel permeation chromatography (GPC)

The molecular weights and molecular weight distribution of polymers were determined on a Waters 717 Plus autosampler gel permeation chromatography apparatus equipped with Waters RH columns and a Dawn Eos (Wyatt Technology) multiangle laser light scattering detector and the measurements were carried out at 25 °C with tetrahydrofuran (THF) as the eluent at the rate of 1.0 mL/min.

3. Results and discussion

3.1. Synthesis of PS-alt-PEO alternating multiblock copolymer

Polystyrene-*block*-poly(ethylene oxide) alternating multiblock copolymer (PS-*alt*-PEO) can be synthesized *via* coupling reaction [47] and redox polymerization [48]. More recently, Huang et al. [49,50] reported that the synthesis of this polymer *via* reversible addition-fragmentation chain transfer (RAFT) of styrene using a trithiocarbonate-embedded PEO macro-chain transfer agent. In this work, the Huisgen 1,3-dipolar cycloaddition reaction (i.e., click chemistry) was used to couple the macromers of azido-terminated PS (N_3-PS-N_3) and propargyl-terminated PEO and the synthetic routes are shown in Scheme 1. The azido-terminated PS was synthesized *via* the substitute reaction between bromo-terminated PS (Br-PS-Br) and sodium azide (NaN_3), i.e., the bromine atoms were substituted by azido groups. The bromo-terminated PS with desired molecular weight was firstly prepared *via* atomic transfer radical polymerization (ATRP) of styrene with dimethyl 2,6-dibromoheptanedioate as the initiator in the presence of the catalytic complex of Cu(I)Br/PMDETA. The propargyl-terminated poly(ethylene oxide) were prepared *via* the reactions between propargyl bromide and poly(ethylene glycol) (PEG) ($M_n = 4000$). To promote the reaction to completion, propargyl bromide was excessive (e.g., two equivalence of terminal hydroxyl groups of PEG) and the reaction was carried out in the presence of sodium hydride. Shown in Fig. 1 are the ^{1}H NMR spectra of the bromo-terminated PS and its derivative after the terminal bromine atoms were substituted by azido groups. The resonance at 4.3–4.65 is ascribed to the methane proton of $BrCHCH_2$ whereas the signals at 3.35–3.6 are assignable to the protons in the structural unit of H_3COCO. It is seen that from with the occurrence of the substitution reaction, the resonance signals of methine protons of bromo-terminated PS was shifted from 4.30–4.60 to 3.8–4.00 ppm. The observation that no remnant signal of proton resonance at 4.30–4.60 ppm for the product indicates that the substitution reaction has been carried out to completion. The molecular weight of the bromo-terminated PS was calculated according to the ratio of integration intensity of methyl ester protons of the initiator to aromatic protons of St structural units to be $M_n = 4900$, which has a good correspondence with the molecular weight obtained from the conversion of the monomer. The transformation of the PEG to propargyl-terminated PEO can be evidenced by Fourier transform infrared (FTIR) and ^{1}H NMR spectroscopy. Shown in Fig. 2 are the FTIR spectra of the poly(ethylene glycol) ($M_n = 4000$) and its derivative with propargyl terminal groups. It is seen that the stretching vibration band of the terminal hydroxyl groups at 3395 cm^{-1} virtually disappeared with the occurrence of the capping reaction; concurrently a new band appeared at 3243 cm^{-1}, which is ascribed to the stretching vibration of C—H bond of alkyne groups. This result can be further confirmed by ^{1}H NMR spectroscopy (see Fig. 3). According to the ratio of integration intensity of alkyne to ethylene protons in the ^{1}H NMR spectra, it is judged that the capping reaction of PEG with alkynyl groups was carried out to completion. The FTIR and ^{1}H NMR spectroscopy indicate that the propargyl-terminated poly(ethylene oxide)s were successfully obtained.

The propargyl-terminated PEO was used to react with the equimolar diazido-terminated PS to polystyrene-*block*-poly(ethylene oxide) alternating block copolymer (PS-*alt*-PEO), i.e., the Huisgen 1,3-dipolar cycloaddition polymerization was carried out in *N*,*N*′-dimethylformamide solution with copper (I) bromide as the catalyst. It is observed that the viscosity of the reactive system was gradually increased with the occurrence of the polymerization, suggesting that the molecular weight of the system was significantly increased. The resulting product was subjected to Fourier transform infrared spectroscopy (FTIR) and the FTIR spectrum of PS-*alt*-PEO alternating multiblock copolymer is presented in Fig. 4. The intense band at 1109 cm^{-1} is attributed to the stretching vibration of C—O bonds in PEO blocks where the band in the range of 2920 cm^{-1} is ascribed to the bending vibration of C—H bonds in the mono-substituted aromatic ring and the bands at 1450–1600 cm^{-1} are ascribed to the bending vibration of C═C of aromatic rings, indicating the presence

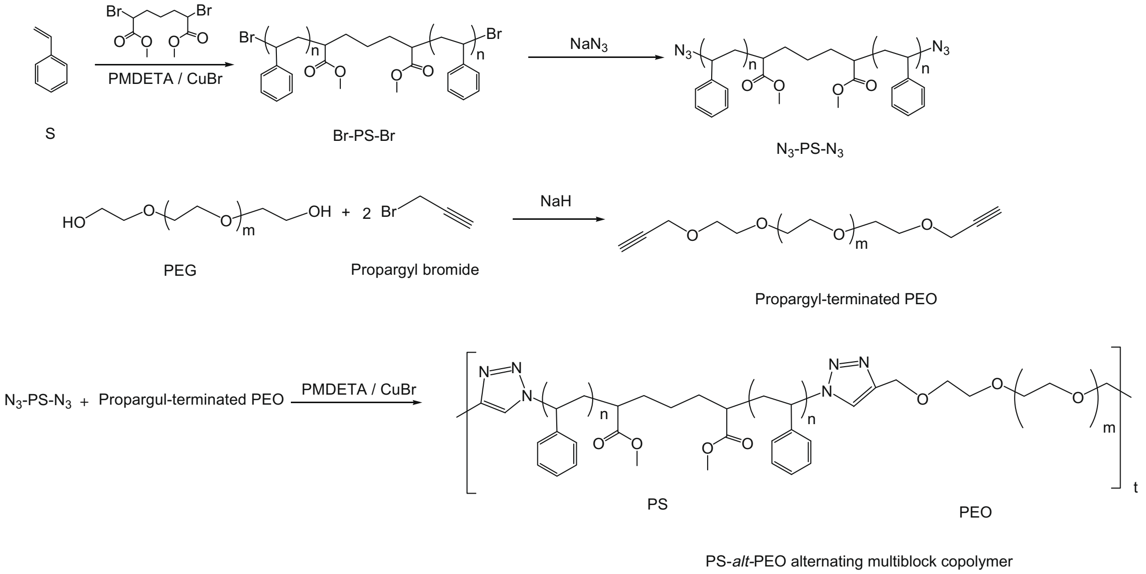

Scheme 1. Synthesis of PS-*alt*-PEO alternating multiblock copolymer.

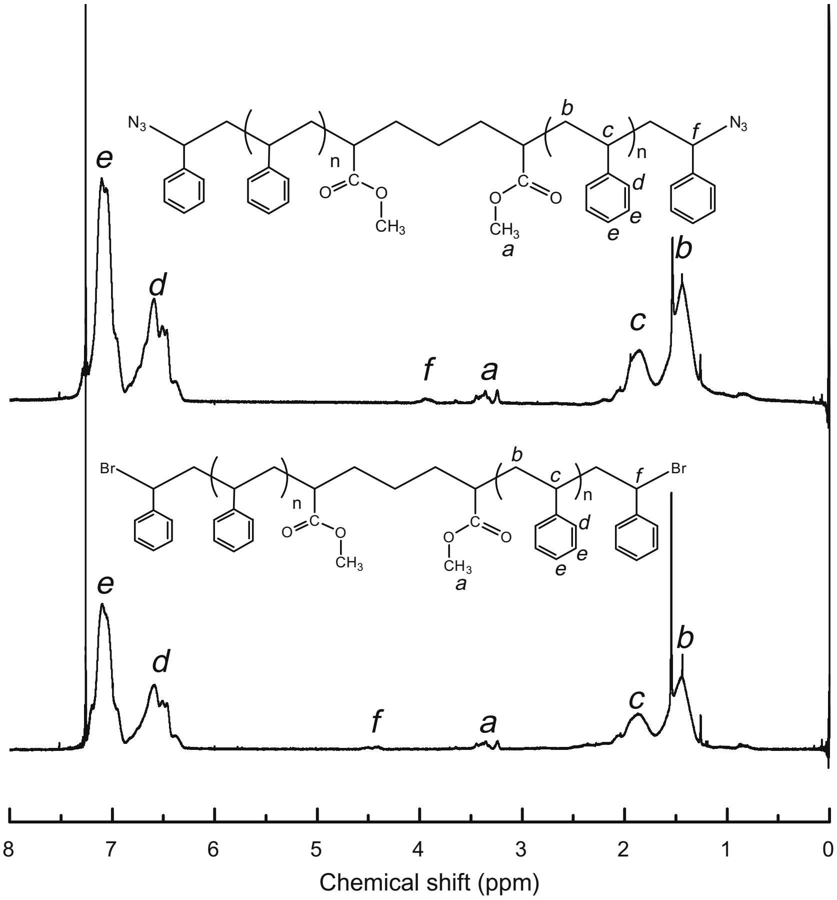

Fig. 1. ^{1}H NMR spectrum of bromo-terminated polystyrene.

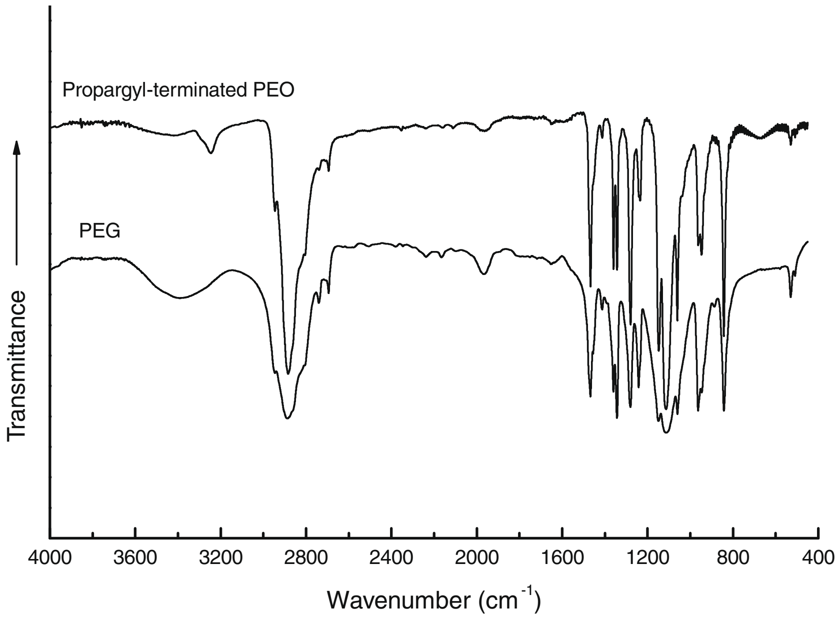

Fig. 2. FTIR spectra of PEG and propargyl-terminated PEO.

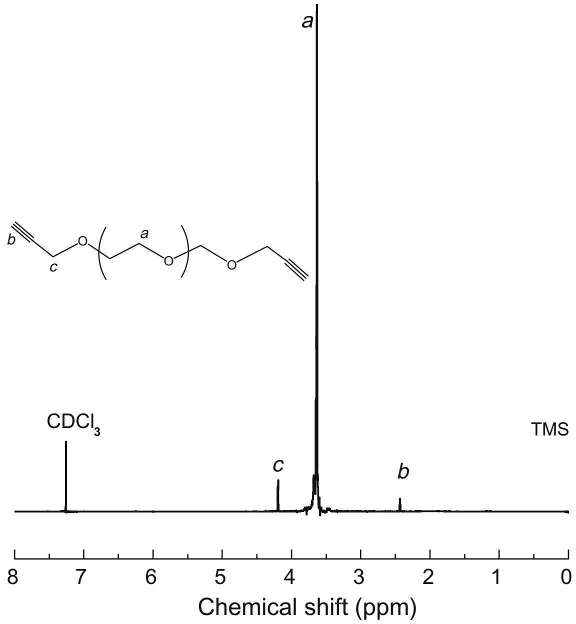

Fig. 3. ^{1}H NMR spectrum of propargyl-terminated PEO.

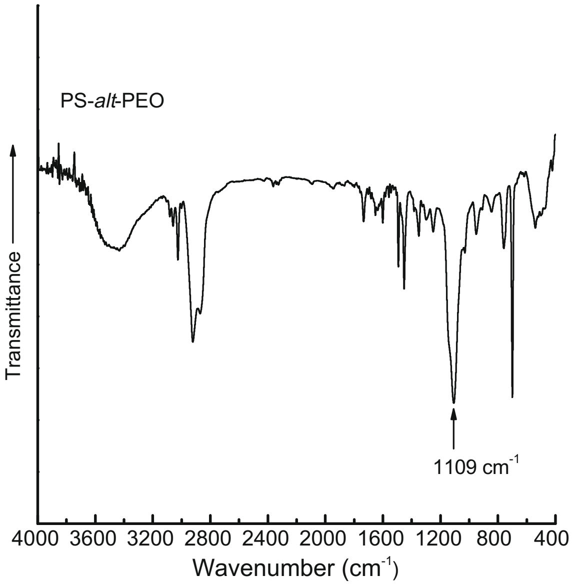

Fig. 4. FTIR spectrum of PS-*alt*-PEO alternating multiblock copolymer.

of PS blocks. In view of the FTIR spectrum it is judged that the resulting polymer combined the structural features from PEO and PS. The occurrence of click polymerization between propargyl-terminated PEO and azido-terminated PS is evidenced by the appearance of the band at 3244 cm^{-1}, which is assignable to stretching vibration of alkynyl groups. This observation was further confirmed with ^{1}H NMR spectroscopy (see Fig. 5), in which the resonances signal of methine protons connected to azido group in PS block at 3.80–4.10 ppm disappeared, instead, the resonance of methine protons connected to triazole moiety appeared at 4.95–5.25 ppm appeared. The gel permeation chromatography (GPC) was employed to measure the molecular weights of the PS-*alt*-PEO alternating multiblock copolymers and the GPC curves were showed in Fig. 6. The GPC curve of the resulting polymer displayed a unimodal peak, suggesting that the polymerization between the two macromers was performed to completion. The PS-*alt*-PEO alternating multiblock copolymer possessed the

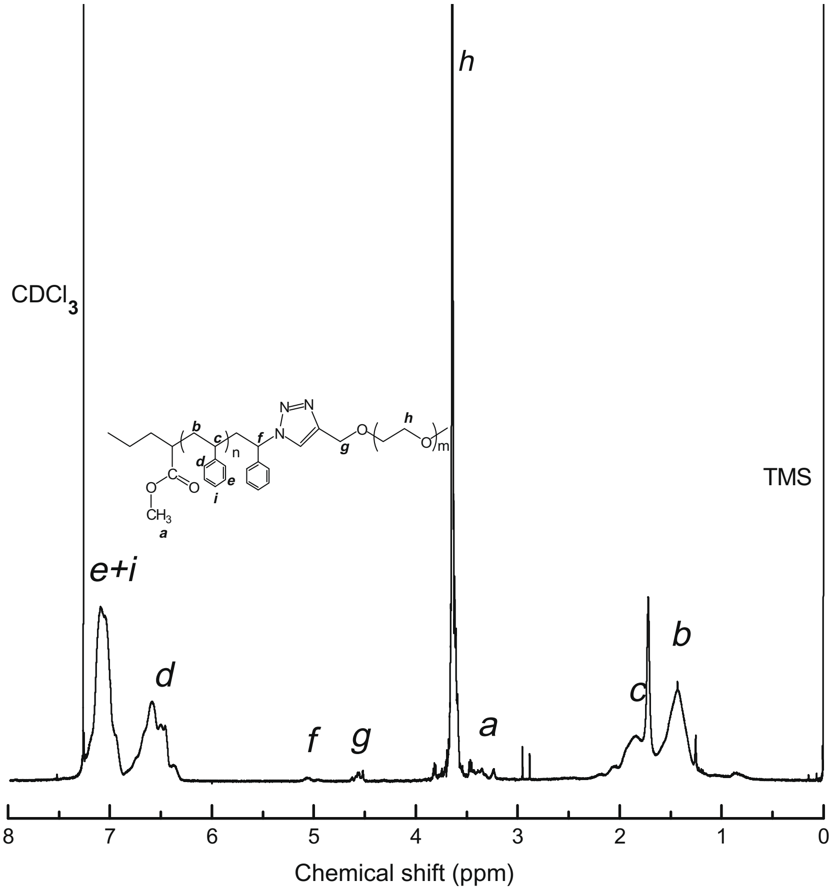

Fig. 5. ^{1}H NMR spectrum of PS-*alt*-PEO alternating multiblock copolymer.

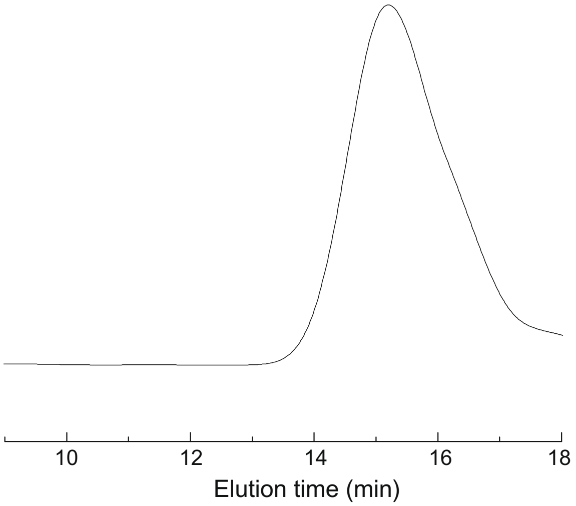

Fig. 6. Gel permeation chromatography (GPC) curve of PS-*alt*-PEO alternating multiblock copolymer.

molecular weights of $M_n = 24{,}700$ and $M_w = 55{,}200$. It should be pointed out that the polydispersity of molecular weights of the alternating block copolymers is 2.23, which is fairly broad, which could be associated with the decreased reactivity of terminal functional groups in the macromers. The similar result was also obtained with the polymerization of the other macromers (or polymers) [26,51].

The PS-*alt*-PEO was subjected to thermal analysis and the DSC curves are presented in Fig. 7. In the first DSC scan, the PS-*alt*-PEO alternating multiblock copolymer displayed a glass transition at −60 °C, an endothermic transition at *c.a.*13 °C and a glass transition at about 50 °C. The glass transition at −60 °C was ascribed to PEO microdomains where the endothermic peak at *c.a.*13 °C was attributed to the melting transition of PEO microdomains. Owing to the short length [i.e., M_n (PS) = 4900], the T_g of the PS domains is a little lower than the value widely reported for PS (*c.a.* 110 °C). The fact that the melting transition appeared prior to the glass transition suggests that the alternating multiblock copolymer is microphase-separated. The observation of melting temperature of PEO block in the multiblock copolymer is much lower than that of the pure PEO (*c.a.* 50 °C) (see Fig. 7b) could be associated to the confined crystallization of PEO in the copolymer. In PS-*alt*-PEO alternating multiblock copolymer, the crystallization of PEO was confined with the nanodomains and the perfection of crystals and the rate of crystallization could be significantly diminished. The decreased rate of crystallization

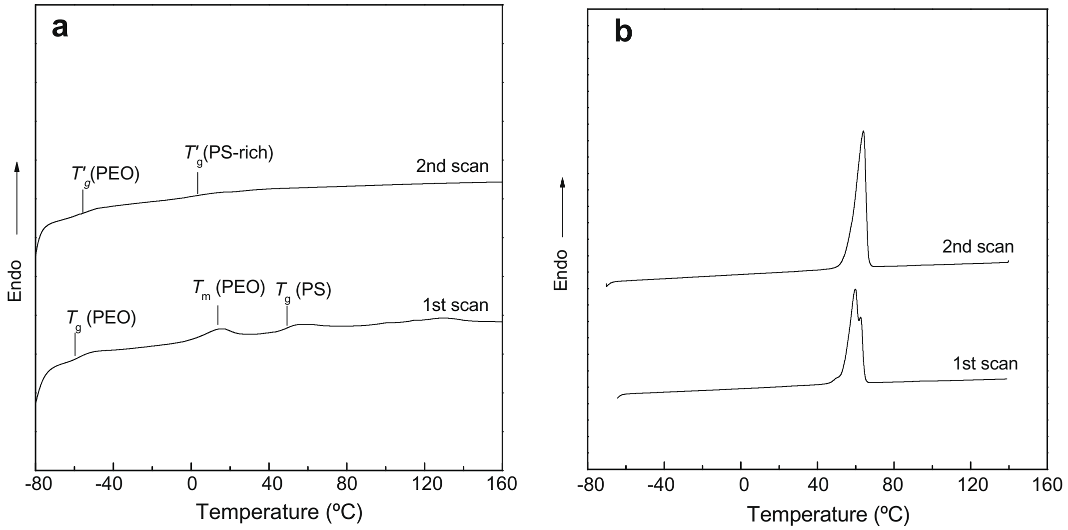

Fig. 7. DSC curves of PS-*alt*-PEO alternating multiblock copolymer (a) and PEG (M_n = 4000) (b).

can be evidenced by the second DSC scan after the sample was quenched from the melt. In the second DSC scan, the melting transition was no longer exhibited in the DSC curves of PS-*alt*-PEO alternating multiblock copolymer in marked contrast to the case of the pure PEG; two glass transitions at −55 °C and a broad one (−30–40 °C) were displayed. The slight increase in T_g of PEO microdomains and the decrease in T_g of PS could result from the partial miscibility of PS and PEO subchains in the block copolymer while the copolymers were thermally annealed at 160 °C. The microphase separation in PS-*alt*-PEO alternating multiblock copolymer can be further evidenced by atomic force microscopy (AFM). Shown in Fig. 8 is the AFM phase image of the alternating multiblock copolymer. It seen that the microphase separation at the nanometer scale occurred and the co-continuous nanophases (dark and light regions) can be ascribed to PS and PEO microdomains, respectively.

3.2. Reaction-induced microphase separation

The PS-*alt*-PEO alternating multiblock copolymer was incorporated into epoxy resin to investigate the reaction-

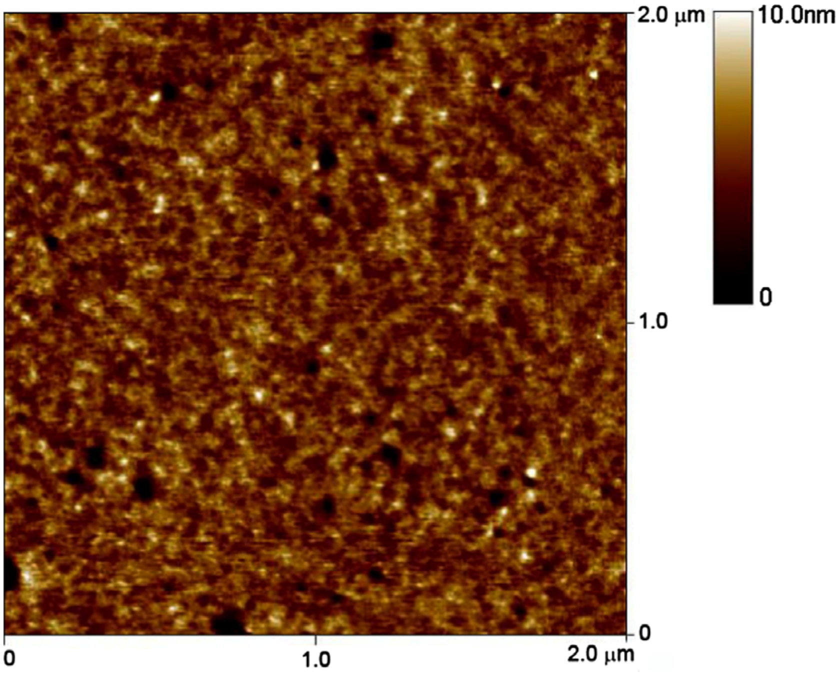

Fig. 8. AFM image of PS-*alt*-PEO alternating multiblock copolymer.

induced microphase separation (RIMS). It has been known that PEO remains soluble up to high conversions and its eventual partial phase separation at high conversions does not affect the formation of nanostructures [7] whereas the mixtures composed of PS and epoxy precursors displayed an upper critical solution temperature (UCST) behavior. It has been known that for the binary mixture of diglycidyl ether of bisphenol A (DGEBA) with PS the upper critical solution temperature can be as high as 90 °C while the molecular weight of PS is $M_n = 7500$ [9]. While the stoichiometric 4,4′-methylenebis (2-chloroaniline) (MOCA) was added to the mixture as the curing agent), the ternary system comprised of DGEBA, MOCA and PS became fully homogenous at room temperature owing to the change in solubility parameter resulting from the incorporation [9]. The reaction-induced phase separation can occur while the curing reaction is carried out at the temperature above the critical solution temperature.

In the present case, the PS-*alt*-PEO alternating multiblock copolymer was incorporated into epoxy resin and the mixtures comprised of DGEBA, MOCA and PS-*alt*-PEO were cured at elevated temperature to obtain the nanostructured thermosets. Before curing, all of the ternary mixtures composed of DGEBA, MOCA and PEG-*alt*-PS were transparent and homogeneous, suggesting that no phase separation occurred. After cured at the elevated temperatures, the epoxy thermosets with the PEG-*alt*-PS contents up to 40 wt.% were obtained. It is seen that all of the cured products investigated are homogeneous and transparent, suggesting that no macroscopic phase separation occurred at the scale exceeding the wavelength of visible lights with the occurrence of curing reaction. It should be pointed out that the clarity does not exclude the possibility of microphase separation in this system. The morphologies of the thermosets were examined by means of atomic force microscopy (AFM) and small-angle X-ray scattering (SAXS).

Shown in Fig. 9 are the AFM micrographs of the thermosets containing PS-*alt*-PEO alternating multiblock copolymer. The left-hand side of each micrograph is topography image and the right the phase image. The topography images showed that the surfaces of the as-prepared specimens are free of visible defects and are quite smooth, and thus the effect of roughness resulting from the specimen trimming on morphology is negligible. It is seen that all the thermosets exhibited microphase-separated morphologies. In terms of the volume fraction of PS and the difference in viscoelastic properties between epoxy matrix and PS phases, the light continuous regions are assignable to the cross-linked epoxy matrix, which was miscible with the PEO blocks of the copolymer while the dark regions are attributed to PS domains. For the thermoset containing 10 wt.% of PS-*alt*-PEO the interconnected PS nanodomains were dispersed in the continuous epoxy matrix (Fig. 9a). With increasing the content of PS-*alt*-PEO, the light nanodomains became coagulated and the size of the nanodomains was increased (Fig. 9b through 9d); both the PS microdomains and the matrix (epoxy + PEO) formed the co-continuous morphology at the nanometer scale. The morphologies of the thermosets containing PS-*alt*-PEO were further investigated by small-angle X-ray scattering (SAXS) and the SAXS profiles are shown in Fig. 10. In the SAXS profile of each thermoset, a single broad scattering shoulder was exhibited, indicating that all the epoxy thermosets are microphase-separated, i.e., the thermosets possessed the nanostructured morphology. The appearance of the sole primary scattering in the each SAXS curve suggests that no long-ranged ordered structured exited in the epoxy thermosets. The result of SAXS is in a good agreement with that of AFM.

3.3. Interpretation of nanostructure formation

In terms of the miscibility of PS and PEO blocks with epoxy resin after and before the curing reaction, it is judged that the formation of nanostructures in thermosets containing PS-*alt*-PEO multiblock copolymer also follows the mechanism of reaction-induced microphase separation as in the epoxy thermosets containing PS-*b*-PEO diblock copolymer [8]. In the nanostructured thermosets, the PEO subchain of the multiblock copolymer remain miscible with epoxy matrix, which can be evidenced by the depression of the glass temperatures (T_g's) of epoxy matrix. The DSC curves of the control epoxy and the nanostructured thermosets containing PS-*alt*-PEO multiblock copolymer are shown in Fig. 11. The glass transition temperature (T_g) of the control epoxy is about 155 °C. Each nanostructured thermoset displayed one T_g in the range of 100–150 °C and another one at *c.a.* 62 °C is discernable, especially while the concentration of PS-*alt*-PEO is more than 30 wt.%. The former is assignable to the epoxy matrix whereas the latter to PS nanodomains. It is seen that the T_g's of the epoxy matrix are decreased with increasing the concentration of PS-*alt*-PEO multiblock copolymer. The decreased T_g is responsible for the plasticization effect of the PEO blocks on the epoxy matrix. In the reactive blending system, the PS blocks of multiblock copolymer are initially miscible with the precursors of epoxy before curing reaction. With the curing reaction proceeding, the PS blocks were gradually demixed from epoxy matrix as the curing reaction proceeded.

The similar glass transition behavior has been found for the nanostructured thermosets containing PS-*b*-PEO diblock copolymer. However, it is noted that the topological structures of block copolymers has a profound impact on the morphologies of the nanostructured thermosets. It has been reported that the reaction-induced microphase separation occurred in the mixture of epoxy resin with PS-*b*-PEO diblock copolymer and the thermosets displayed long-ranged ordered nanostructures. In this work, a PS-*b*-PEO diblock copolymer which has the similar volume fraction of PS (and/or PEO) subchain was synthesized (see Section 2) and the PS-*b*-PEO diblock copolymer was incorporated into epoxy to investigate the formation of nanostructures in the thermosets. Shown in Fig. 12 are the SAXS profiles of the epoxy thermosets containing PS-*b*-PEO diblock copolymer. It is seen that the well-defined scattering peaks were observed in all the cases, indicating that the thermosets containing PS-*b*-PEO are microphase-separated. In addition, it is seen that all the epoxy thermosets displayed the multiple scattering maxima as denoted with the arrows, indicating that the epoxy thermosets possess long-range ordered nanostructures. This result can

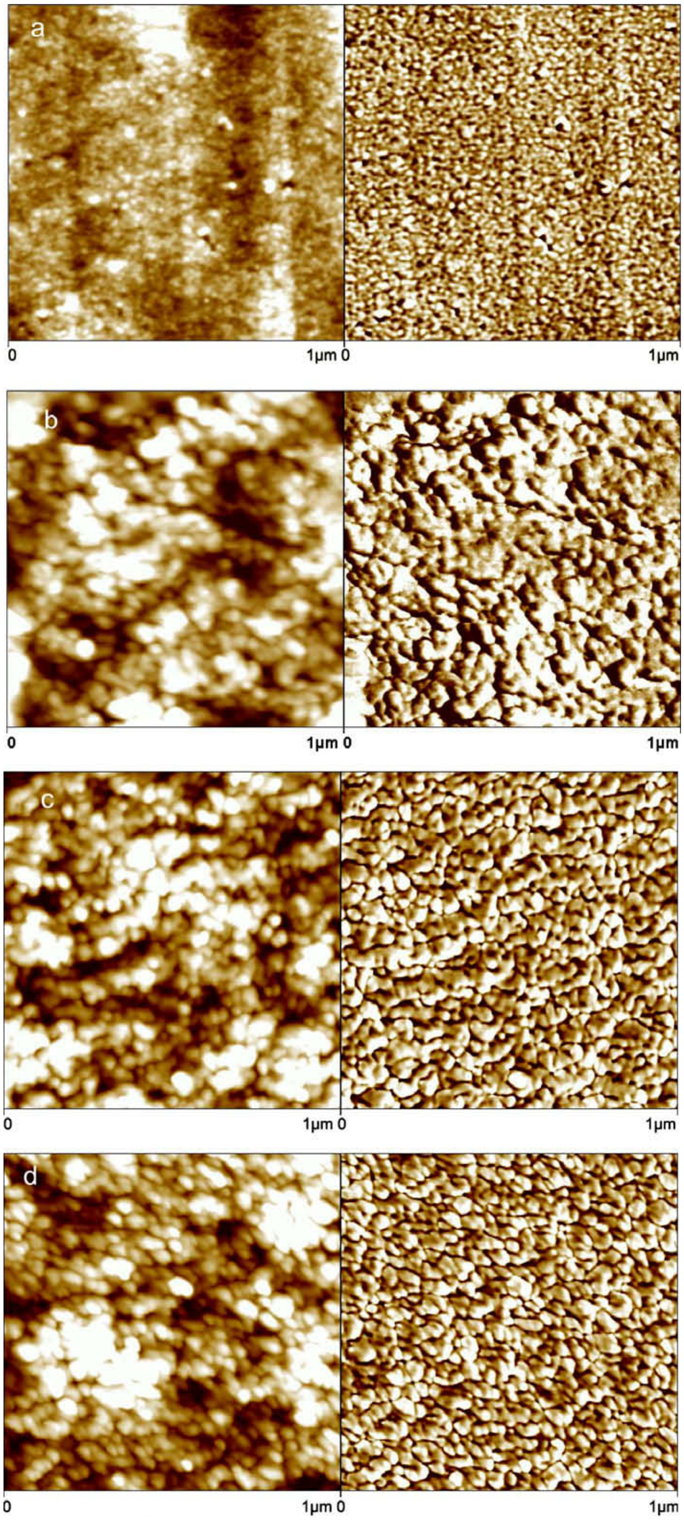

Fig. 9. AFM images of the thermosets containing (a) 10, (b) 20, (c) 30 and (d) 40 wt.% of PS-*alt*-PEO alternating multiblock copolymer. Left: topography. Right: phase contrast images.

further be evidenced by atomic force microscopy as shown in Fig. 13. It should be pointed out that it is not easy unambiguously to judge the types of packing lattices only in terms of SAXS profiles for the thermosetting blends con-

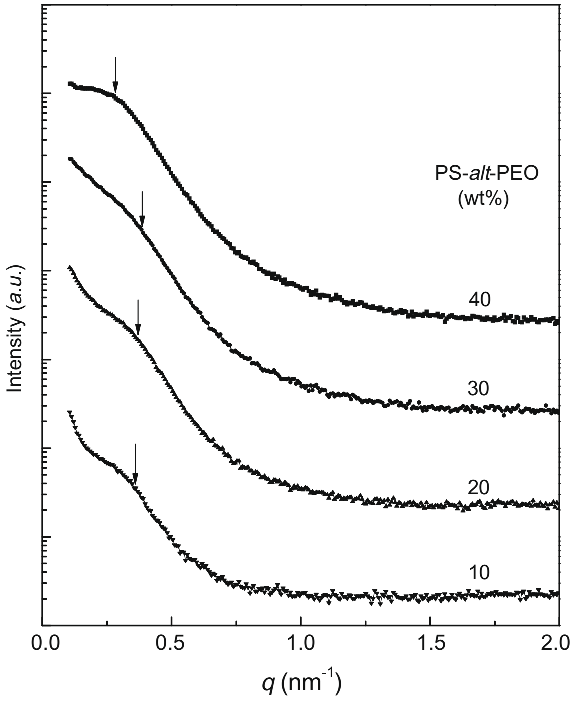

Fig. 10. SAXS profiles of epoxy thermosets containing PS-*alt*-PEO alternating multiblock copolymer.

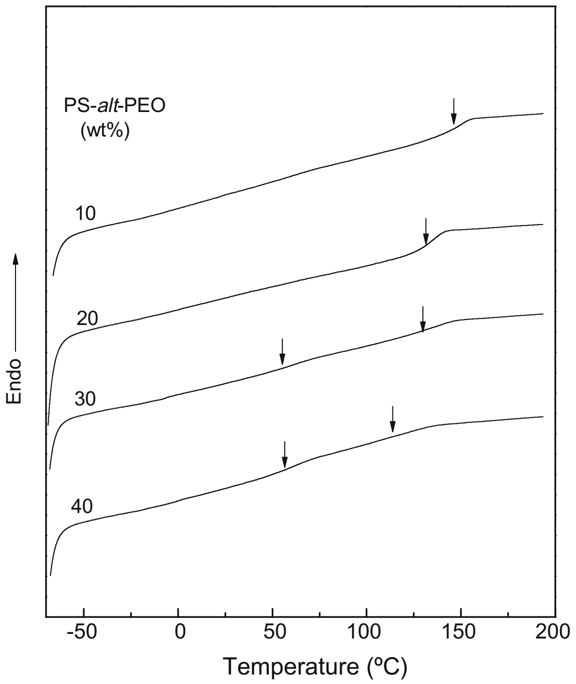

Fig. 11. DSC curves of the epoxy thermosets containing PS-*alt*-PEO alternating multiblock copolymer.

taining 20, 30 wt.% PS-*b*-PEO since the scattering peaks are quite broad, i.e., the ordering is apparently not good enough.

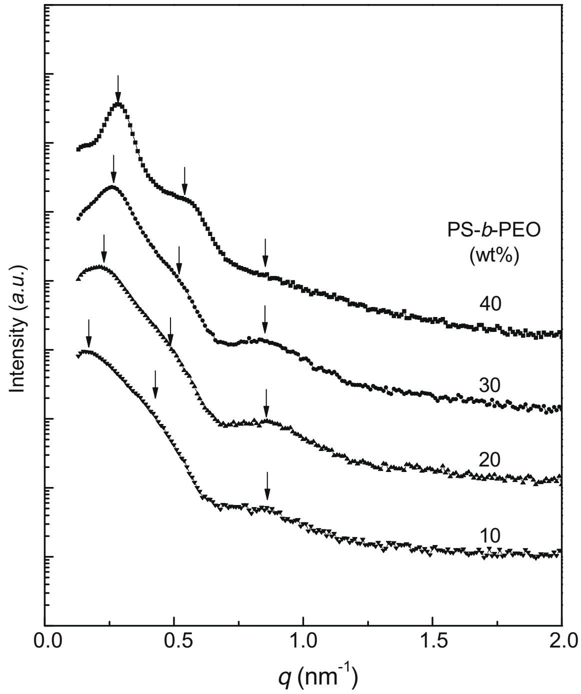

Fig. 12. SAXS profiles of epoxy thermosets containing PS-*b*-PEO diblock copolymer.

The long-ranged ordered nanostructures in epoxy thermosets containing PS-*b*-PEO diblock copolymer is in marked contrast to those of epoxy thermosets containing PS-*alt*-PEO alternating multiblock copolymer. It is proposed that the formation of the long-ranged ordered nanostructures results from the specific topology of the block copolymer (i.e., diblock). The diblock topology of the copolymer could exert little restriction on the ordered arrangement of PS nanodomains in epoxy matrix during the curing reaction since each PS block possesses one free end. It should be pointed out that since the subchains of block copolymer (i.e., PS and PEO) are synthesized in the fashions of living polymerization (i.e., ATRP and cationic polymerization), the polydispersity of length for the blocks are quite narrow, which would promote the formation of uniform PS microdomains with the occurrence of reaction-induced microphase separation. When densely packed, these uniform PS microdomains are capable of forming an ordered dispersion in continuous epoxy matrix. However, in the thermosetting blends of epoxy with PS-*alt*-PEO multiblock copolymer, the reaction-induced microphase separation of PS block is in a more restricted fashion than in the systems containing PS-*b*-PEO diblock copolymer since both terminal ends of PS were bonded with miscible PEO blocks. It is plausible to propose that the coarsening and mobility of PS microdomains were significantly lower than that of the system containing PS-*b*-PEO. In addition, the competitive kinetics between RIMS and polymerization in the thermosetting blends containing PS-*alt*-PEO multiblock copolymer could be quite different from that in the system containing PS-*b*-PEO diblock copolymer since the molecular weight of PS-*alt*-PEO

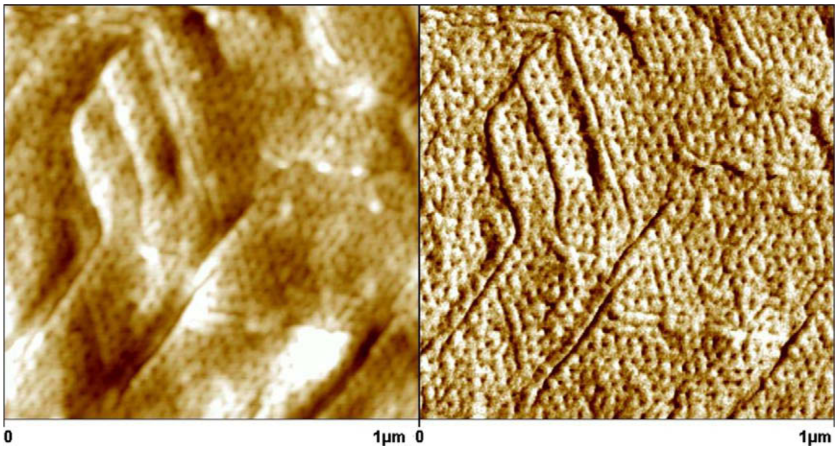

Fig. 13. AFM image of epoxy thermoset containing 40 wt.% PS-*b*-PEO diblock copolymer.

multiblock copolymer ($M_n = 24,700$) is much higher than that of PS-*b*-PEO diblock copolymer ($M_n = 10,100$). The above factors could be unfavorable to the formation of long-ranged ordered arrangement in the epoxy matrix.

4. Conclusions

The PS-*alt*-PEO alternating multiblock copolymer was synthesized by combining atom transfer radical polymerization and click chemistry. The copolymer has been characterized by means of Fourier transform infrared spectroscopy (FTIR), ^{1}H nuclear magnetic resonance spectroscopy (NMR), gel permeation chromatography (GPC) and differential scanning calorimetry (DSC). The PS-*alt*-PEO alternating multiblock copolymer was incorporated into epoxy resin to investigate the behavior of reaction-induced microphase separation, which has been compared to the case of thermosets containing PS-*b*-PEO diblock copolymer. The morphology of epoxy thermosets containing PS-*alt*-PEO alternating multiblock copolymer were investigated by means of atomic force microscopy (AFM), and small-angle X-ray scattering (SAXS) and the nanostructures were detected in all the thermosetting blends investigated. In marked contrast to the case of the thermosets containing PS-*b*-PEO diblock copolymer, the thermosets containing PS-*alt*-PEO multiblock copolymer displayed disordered nanostructures, which have been interpreted on the basis of the restriction of the alternating multiblock topology of the block copolymer on the formation of the nanostructures *via* reaction-induced microphase separation.

Acknowledgments

The financial supports from Natural Science Foundation of China (No. 20474038 and 50873059) and National Basic Research Program of China (No. 2009CB930400) are acknowledged. The authors thank the Shanghai Synchrotron Radiation Facility (SSRF) under the project of 08sr0157 and Shanghai Leading Academic Discipline Project under the project of B202 for the partial supports.

References

[1] Pascault JP, Williams RJJ. In: Paul DR, Bucknall CB, editors. Polymer blends, vol. 1. New York: Wiley; 2000. p. 379–415.
[2] de Gennes PG. Scale concepts in polymer physics. Ithaca, NY: Cornell University Press; 1979.
[3] de Gennes PG. Phys Lett 1969;28A:725.
[4] Ruiz-Pérez L, Royston GJ, Fairclough JA, Ryan AJ. Polymer 2008;49:4475.
[5] Zheng S. In: Pascault JP, Williams RJ, editors. Epoxy polymers: new materials and innovations. Wiley-VCH; 2010 [chapter 5].
[6] Hillmyer MA, Lipic PM, Hajduk DA, Almdal K, Bates FS. J Am Chem Soc 1997;119:2749.
[7] Lipic PM, Bates FS, Hillmyer MA. J Am Chem Soc 1998;120:8963.
[8] Meng F, Zheng S, Zhang W, Li H, Liang Q. Macromolecules 2006;39:711.
[9] Meng F, Zheng S, Li H, Liang Q, Liu T. Macromolecules 2006;39:5072.
[10] Mijovic J, Shen M, Sy JW, Mondragon I. Macromolecules 2000;33:5235.
[11] Grubbs RB, Dean JM, Broz ME, Bates FS. Macromolecules 2000;33:9522.
[12] Kosonen H, Ruokolainen J, Nyholm P, Ikkala O. Macromolecules 2001;34:3046.
[13] Guo Q, Thomann R, Gronski W. Macromolecules 2002;35:3133.
[14] Ritzenthaler S, Court F, Girard-Reydet E, Leibler L, Pascault JP. Macromolecules 2002;35:6245.
[15] Ritzenthaler S, Court F, Girard-Reydet E, Leibler L, Pascault JP. Macromolecules 2003;36:118.
[16] Rebizant V, Abetz V, Tournihac T, Court F, Leibler L. Macromolecules 2003;36:9889.
[17] Dean JM, Verghese NE, Pham HQ, Bates FS. Macromolecules 2003;36:9267.
[18] Rebizant V, Venet AS, Tournillhac F, Girard-Reydet E, Navarro C, Pascault JP, et al. Macromolecules 2004;37:8017.
[19] Dean JM, Grubbs RB, Saad W, Cook RF, Bates FS. J Polym Sci B Polym Phys 2003;41:2444.
[20] Wu J, Thio YS, Bates FS. J Polym Sci B Polym Phys 2005;43:1950.
[21] Zucchi IA, Galante MJ, Williams RJJ. Polymer 2005;46:2603.
[22] Thio YS, Wu J, Bates FS. Macromolecules 2006;39:7187.
[23] Serrano E, Tercjak A, Kortaberria G, Pomposo JA, Mecerreyes D, Zafeiropoulos NE, et al. Macromolecules 2006;39:2254.
[24] Ocando C, Serrano E, Tercjak A, Pen~a C, Kortaberría G, Calberg C, et al. Macromolecules 2007;40:4068.
[25] Maiez-Tribut S, Pascault JP, Soulé ER, Borrajo J, Williams RJJ. Macromolecules 2007;40:1268.
[26] Gong W, Zeng K, Wang L, Zheng S. Polymer 2008;49:3318.
[27] Dean JM, Lipic PM, Grubbs RB, Cook RF, Bates FS. J Polym Sci B Polym Phys 2001;39:2996.
[28] Serrano E, Tercjak A, Kortaberria G, Pomposo JA, Mecerreyes D, Zafeiropoulos NE, et al. Macromolecules 2006;39:2254.
[29] Meng F, Zheng S, Liu T. Polymer 2006;47:7590.
[30] Sinturel C, Vayer M, Erre R, Amenitsch H. Macromolecules 2007;40:2532.

[31] Ocando C, Serrano E, Tercjak A, Pena C, Kortaberria G, Calberg C, et al. Macromolecules 2007;40:4068.
[32] Xu Z, Zheng S. Macromolecules 2007;40:2548.
[33] Meng F, Xu Z, Zheng S. Macromolecules 2008;41:1411.
[34] Fan W, Zheng S. Polymer 2008;49:3157.
[35] Fan W, Wang L, Zheng S. Macromolecules 2009;42:327.
[36] Yi F, Zheng S. J Phys Chem B 2009;113:1857.
[37] Liu J, Sue HJ, Thompson ZJ, Bates FS, Dettloff M, Jacob G, et al. Acta Mater 2009;57:2691.
[38] Thompson ZJ, Hillmyer MA, Liu J, Sue HJ, Dettloff M, Bates FS. Macromolecules 2009;42:2333.
[39] Liu J, Sue HJ, Thompson ZJ, Bates FS, Dettloff M, Jacob G, et al. Macromolecules 2008;41:7616.
[40] Odian G. Principles of polymerization. 4th ed. New York: John Wiley & Sons, Inc.; 2004.
[41] Rostovtsev VV, Green LG, Fokin VV, Sharpless KB. Angew Chem Int Ed 2002;41:2596.
[42] Binder WH, Sachsenhofer R. Macromol Rapid Commun 2007;28:15.
[43] Nandivada H, Jiang X, Lahann J. Adv Mater 2007;19:2197.
[44] Lutz JF. Angew Chem Int Ed 2007;46:1018.
[45] Gao H, Louche G, Sumerlin BS, Jahed N, Golas P, Matyjaszewski K. Macromolecules 2005;38:8979.
[46] Jnkova K, Chen X, Kops J, Batsberg W. Macromolecules 1998;31:538.
[47] Shimura Y, Lin SJ. Polym Sci A Polym Chem 1970;18:2171.
[48] Cakmak I. Angew Makromol Chem 1995;224:49.
[49] Jia Z, Liu C, Huang. J Polym 2006;47:7615.
[50] Jia Z, Xu X, Fu Q, Huang J. J Polym Sci A Polym Chem 2006;44:6071.
[51] Hargadon MT, Davey EA, McIntyre TB, Gnanamgari D, Wynne CM, Swift RC, et al. Macromolecules 2008;41:741.